Tunable Nanoresonators Constructed from Telescoping Nanotubes

K. Jensen,* Ç. Girit, W. Mickelson, and A. Zettl†

Department of Physics, University of California at Berkeley, Center of Integrated Nanomechanical Systems, University of California at Berkeley, The Molecular Foundry, Lawrence Berkeley National Laboratory, and Materials Sciences Division, Lawrence Berkeley National Laboratory, Berkeley, California 94720, USA

(Received 20 January 2006; published 31 May 2006)

We have created a tunable mechanical nanoscale resonator with potential applications in precise mass, force, position, and frequency measurement. The device consists of a specially prepared multiwalled carbon nanotube (MWNT) suspended between a metal electrode and a mobile, piezo-controlled contact. By exploiting the unique telescoping ability of MWNTs, we controllably slide an inner nanotube core from its outer nanotube casing, effectively changing its length and tuning its flexural resonance frequency.

DOI: 10.1103/PhysRevLett.96.215503 PACS numbers: 85.35.Kt, 61.46.Fg

Nanoscale resonators, with their low masses, low force constants, and high resonant frequencies, are capable of weighing single bacteria [1], detecting single spins in magnetic resonance systems [2], and even probing quantum mechanics in macroscopic systems [3,4]. These resonators are typically created from surface-micromachined silicon. Carbon nanotubes provide an alternate, nearly ideal building material because of their low density, high Young's modulus, and atomically perfect structure. Already there has been progress in analyzing and constructing nanotube-based resonators [5–7]. However, current designs either operate at a single frequency or have a relatively narrow frequency range, possibly limiting their application.

We propose a fundamentally different nanotube resonator, which takes advantage of one of carbon nanotubes' most interesting properties. Multiwalled carbon nanotubes (MWNTs), which consist of multiple, concentric nanotubes precisely nested within one another, exhibit a striking telescoping property whereby an inner nanotube core may slide within the atomically smooth casing of an outer nanotube shell [8]. This property has been exploited to build a rotational nanomotor [9] and a nanorheostat [10]. Future nanomachines such as a gigahertz mechanical oscillators are envisioned [11]. By harnessing this versatile telescoping property in a new fashion, we have created a tunable nanoscale resonator operating at frequencies up to 300 MHz and tunable over a range of more than 100 MHz. Relatively high quality factors (up to 1000) indicate that sliding friction between telescoping sections of our resonator is an insignificant source of dissipation, and in fact the telescoping action may increase quality factors through the suppression of thermoelastic dissipation.

Figure 1(a) is a schematic drawing of our tunable nanoresonator. A MWNT is suspended between a stationary metal electrode and a mobile, piezo-controlled contact, similarly to previous experiments [10]. To create this geometry, a macroscopic fiber of arc-grown MWNTs is fixed via conductive epoxy to a platinum wire, which serves as the stationary electrode. Using a nanomanipulation platform (Nanofactory Instruments AB), it is possible to approach and contact an individual MWNT, protruding from the fiber, with an etched tungsten tip (i.e., the mobile contact). Because of the van der Waals attraction between MWNTs, protruding MWNTs are sometimes solidly bundled with other MWNTs; however, even in these cases, it is still possible to contact a single MWNT and construct the device. By peeling the outer shell of the MWNT [12] and exposing the inner core, we access the MWNT's unique telescoping function. Then, like a trombone player shifting notes, we controllably slide the inner nanotube from its casing using the mobile contact, effectively changing the length of the MWNT and tuning its resonant frequency. In the top image, the resonator is fully retracted and has a relatively high resonant frequency. In the bottom image, the resonator is extended and consequently has a lower resonant frequency. By operating the device in an external magnetic field and applying an alternating electrical current through the MWNT, we can excite the mechanical vibrations of the nanotube via the Lorentz force [13]. With a transmission electron microscope (TEM) it is possible to detect these vibrations through the physical displacement of the nanotube. Our experiments were conducted at room temperature and in a magnetic field, provided by the TEM objective lens, of approximately 1.3 T [14].

Transmission electron micrographs in Fig. 1(b) show our tunable nanoresonator in action. The dark region on the right is the mobile contact, while the stationary clamp is more than 200 nm off the image to the left. Note that the bulge on the nanotube shown in the left portion of the image is not the clamp but rather the beginning of a MWNT bundle. The first two images show a 558 nm long nanotube beam before resonance (sharp) and during resonance at 225.0 MHz (blurred). The final two images show the nanotube beam after the inner nanotube has been telescoped out 50 nm. The resonant frequency has shifted downward to 192.7 MHz.

Resonance peaks are detected by sweeping the driving frequency through the fundamental resonant frequency of the device and afterward analyzing video from the TEM

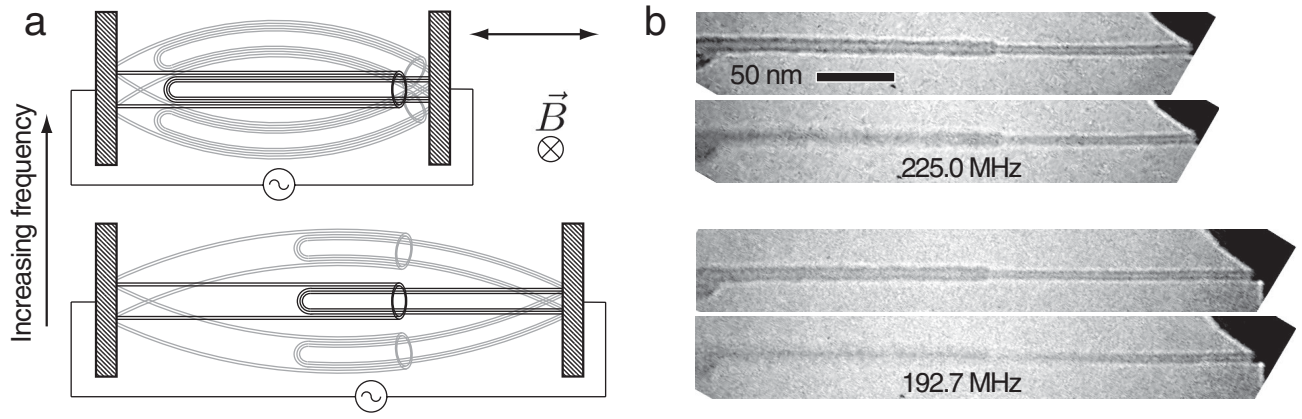

FIG. 1. (a) Schematic drawing of our tunable resonator. A specially prepared MWNT is suspended between a stationary contact and mobile, piezo-controlled electrode. Varying the length of the nanotube beam through the controlled telescoping of the inner nanotube core from the outer nanotube shell tunes its resonant frequency. Operating the device in an external magnetic field, B, allows actuation with alternating current via the Lorentz force. (b) TEM micrographs show the device in action. The dark region on the right is the mobile contact, while the stationary clamp is more than 200 nm off the image to the left (the bulge pictured at the left of the image is actually the beginning of a MWNT bundle). The top two images show the nanotube at one extension off resonance (sharp) and on resonance (blurred) with a resonant frequency $f = 225.0$ MHz. The bottom two images show an extended nanotube with a lowered resonant frequency (192.7 MHz).

with an image processing routine. Resonance in the fundamental mode, as opposed to higher order modes, is confirmed by sweeping the frequency upward from 100 kHz (below any conceivable resonance) and stopping at the first resonance. The maximum displacement of the visible portion of the nanotube is determined to within 0.2 nm for each video frame. A Lorentzian is fit to the data to determine the resonant frequency and quality factor. The inset in Fig. 2 shows a typical resonance response of our nanoresonator with a quality factor of 620. Note that measured quality factors may actually be up to 10% lower than intrinsic values due to inherent dissipation in our measurement apparatus caused by eddy currents created by vibrating the nanotube in a magnetic field [15]. Despite this fact, quality factors for our devices were generally between 100 and 1000, relatively high compared to other doubly clamped nanotube resonators [6].

To demonstrate our ability to tune the nanoresonator, we plot resonant frequency versus beam extension for four devices in Fig. 2. As expected, extended nanotubes produce lower frequencies. Also, each device covers a relatively wide range of frequencies, and together the devices span nearly the entire spectrum from 30 MHz to 300 MHz. Apparent in the graph is the extreme sensitivity of resonant frequency to telescoping extension, more than 1 MHz/nm for one device, suggesting possible application as a precision distance or position sensor or strain gauge.

Euler-Bernoulli beam theory describes how frequency varies with beam extension. The nanotube beam is treated as a continuum, elastic medium subject to the differential equation:

$$\frac{\partial^2}{\partial x^2}\left(EI\frac{\partial^2 y}{\partial x^2}\right) - \frac{\partial}{\partial x}\left(T\frac{\partial y}{\partial x}\right) = -\rho A\frac{\partial^2 y}{\partial t^2}, \qquad (1)$$

where $y(x)$ is the transverse displacement of the beam along its length, E is the Young's modulus, I is the areal moment of inertia, T is the tension, ρ is the density, and A is the cross-sectional area [16]. For a cylindrical beam with outer and inner radii, r_{outer} and r_{inner}, $I = \pi(r_{\text{outer}}^4 - r_{\text{inner}}^4)/4$. Strictly speaking our device is not a simple cylindrical beam but rather is more closely modeled as a combination of two cylindrical beams, the shell nanotube combination and the core nanotube combination. In some cases, the shell nanotube combination is a member of a MWNT bundle further complicating matters. To simplify

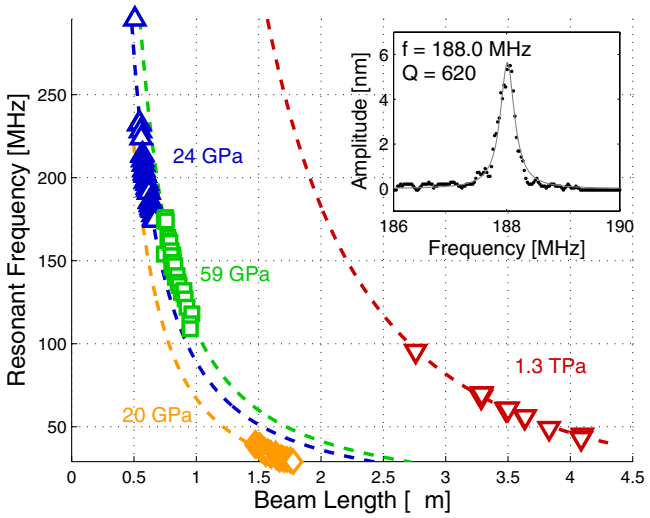

FIG. 2 (color online). Tuning curves for four nanoresonator devices. A theoretical model provides a good fit to the data and yields reasonable values for the effective Young's modulus of each device. The inset shows a typical resonance peak with a Lorentzian fit.

analysis, however, the system is here modeled as a simple cylindrical beam with effective values of E, I, ρ, A, r_{outer}, and r_{inner} which remain constant over the length of the beam and during operation. Applying the boundary conditions of a doubly clamped system with beam length, l ($y(0) = 0$, $y'(0) = 0$, $y(l) = 0$, $y'(l) = 0$) and solving the equation for the resonant frequency of the fundamental mode gives [16]

$$f_0 \approx \frac{22.4}{2\pi l^2}\sqrt{\frac{EI + 0.024Tl^2}{\rho A}}. \quad (2)$$

Numerical solutions of Eq. (1) using the more complicated two-cylinder and MWNT bundle models indicate that this approximate solution is accurate to within 5% for typical devices over their entire range of operation.

Tension in our device is supplied by the van der Waals attraction between the core nanotube and its shell, $F_{\text{vdw}} = (0.2\ \text{J/m}^2)C$, where C is the core nanotube's circumference [8]. Interestingly, as a result, tension remains constant regardless of extension, temperature, or other environmental factors, allowing robust and reproducible results.

The measured maximum transverse displacement of our devices as a function of position is consistent with that of a doubly clamped beam vibrating in its fundamental mode. Using Eq. (2) to calculate f_0, we fit curves to the experimental tuning data in Fig. 2. Only the Young's modulus and an offset to the length of the beam were used as fitting parameters. Because of our current fabrication techniques, some of our tunable nanoresonators are composed of nanotube bundles rather than individual nanotubes resulting in lower values for the effective Young's modulus, which may vary from one device to another. Also, the exact location of the sample-side clamp is often obscured in TEM imaging requiring the usage of a length offset. Specifically, we directly measure the change in length of the beam and determine the total length through the fitting parameter. The plots in Fig. 2 show frequency versus the entire fitted length. The data follow the curves well and give reasonable values for the Young's modulus of a MWNT (1.3 TPa) [17] or MWNT bundles (20 GPa, 24 GPa, and 59 GPa) [18].

As well as having many practical applications, our tunable resonator also provides an excellent platform for studying the physics of dissipation. Figure 3 is a plot of energy dissipation (Q^{-1}) as a function of extension for one device. There appears to be a significant (p value $= 0.03$) positive correlation between dissipation and extension. Possible dissipation mechanisms include eddy current damping, clamping loss, thermoelastic effects, core-shell sliding friction, and various irreversible processes involving surface defects and adsorbents. Eddy current damping [15], though it would exhibit a positive correlation with extension, cannot account for the magnitude of the increase in dissipation. Clamping loss and thermoelastic dissipation both have a frequency dependence that would cause dissipation to decrease as length increases, opposite to what is observed [19]. Moreover, thermoelastic dissipation is likely greatly suppressed because the nanotube may telescope to increase its length rather than stretch. Sliding friction could depend on overlap length between the core nanotube and shell nanotube; however, again, dissipation would likely decrease with increased extension because there would be less overlap [20]. Surface losses therefore remain the most likely candidate for the dominant form of dissipation here. This important size-dependent contributor to dissipation has been suspected in other nanoscale oscillators [21].

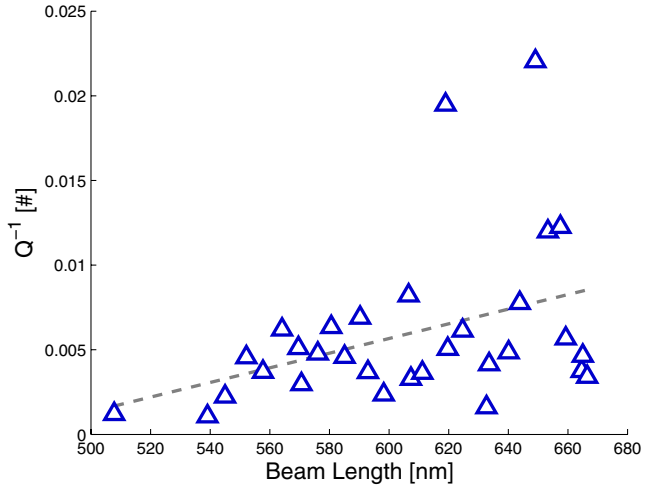

FIG. 3 (color online). Dissipation as a function of nanotube beam length for one device. A linear regression indicating a significant positive correlation provides evidence for length-dependent dissipation.

Surface losses are typically modeled through the addition of a thin dissipative layer to the resonator's surface. Though our experiments were conducted in high vacuum (10^{-7} torr), the surface of the nanotube, even the newly exposed portion following telescoping, is likely covered with more than a monolayer of adsorbents, which functions as the dissipative layer. Dissipation, defined as the inverse of the quality factor, is given by: $Q^{-1} = \Delta W/W_0$, where ΔW is the energy lost per cycle and W_0 is the energy originally stored in the resonator. Stored energy is related to total resonator volume while energy lost per cycle is related to the volume of the dissipative surface layer, resulting in dissipation proportional to the surface-to-volume ratio. Thus, in most nanoscale resonators, dissipation is inversely proportional to length [22]. Curiously, in our nanoresonator, the actual volume of the resonator remains constant during extension giving a dissipation that is directly proportional to length, $Q^{-1} \propto S/V \propto l$.

Our unique high-Q tunable nanoresonator exhibits promise as a precise mass, force, position, or frequency sensor. It has demonstrated a wider frequency range than competing tunable nanoresonator designs. Also, its unique sliding ability lends itself to position sensing applications unlike other immobile resonators. Finally, its nearly perfect atomic structure and precisely controlled geometry make it an ideal tool to study the physics of dissipation.

This work was supported in part by the Director, Office of Energy Research, Office of Basic Energy Sciences, Materials Sciences Division of the US Department of Energy under Contract No. DE-AC-03-76SF00098 and by the National Science Foundation under Grant No. CMS-0510823 and Grant No. EEC-0425914, through the Center of Integrated Nanomechanical Systems.

*Electronic address: kjensen@alum.mit.edu
†Electronic address: azettl@berkeley.edu

[1] B. Ilic, D. Czaplewski, H. G. Craighead, P. Neuzil, C. Campagnolo, and C. Batt, Appl. Phys. Lett. **77**, 450 (2000).
[2] D. Rugar, R. Budakian, H. J. Mamin, and B. W. Chui, Nature (London) **430**, 329 (2004).
[3] M. D. LaHaye, O. Buu, B. Camarota, and K. C. Schwab, Science **304**, 74 (2004).
[4] G. Bressi, G. Carugno, R. Onofrio, and G. Ruoso, Phys. Rev. Lett. **88**, 041804 (2002).
[5] C. Li and T.-W. Chou, Appl. Phys. Lett. **84**, 5246 (2004).
[6] V. Sazonova, Y. Yaish, H. Ustunel, D. Roundy, T. A. Arias, and P. L. McEuen, Nature (London) **431**, 284 (2004).
[7] S. T. Purcell, P. Vincent, C. Journet, and Vu Thien Binh, Phys. Rev. Lett. **89**, 276103 (2002).
[8] J. Cumings and A. Zettl, Science **289**, 602 (2000).
[9] A. M. Fennimore, T. D. Yuzvinsky, W. Q. Han, M. S. Fuhrer, J. Cumings, and A. Zettl, Nature (London) **424**, 408 (2003).
[10] J. Cumings and A. Zettl, Phys. Rev. Lett. **93**, 086801 (2004).
[11] Q. Zheng and Q. Jiang, Phys. Rev. Lett. **88**, 045503 (2002).
[12] J. Cumings, P. G. Collins, and A. Zettl, Nature (London) **406**, 586 (2000).
[13] A. N. Cleland and M. L. Roukes, Appl. Phys. Lett. **69**, 2653 (1996).
[14] M. Kawasaki, JEOL, Inc. (private communication).
[15] A. N. Cleland and M. L. Roukes, Sensors and Actuators A - Physical **72**, 256 (1999).
[16] R. V. Southwell, *An Introduction to the Theory of Elasticity for Engineers and Physicists*, edited by R. V. Southwell (Dover, New York, 1969), illus. 21 cm, reprint of the 1941 ed.
[17] P. Poncharal, Z. L. Wang, D. Ugarte, and W. A. de Heer, Science **283**, 1513 (1999).
[18] A. B. Dalton, S. Collins, E. Munoz, J. M. Razal, V. H. Ebron, J. P. Ferraris, J. N. Coleman, B. G. Kim, and R. H. Baughman, Nature (London) **423**, 703 (2003).
[19] V. B. Braginski, C. Eller, K. S. Thorne, V. I. Panov, and V. P. Mitrofanov, *Systems with Small Dissipation* (University of Chicago Press, Chicago, 1985).
[20] B. N. J. Persson, *Sliding Friction: Physical Principles and Applications, Nanoscience and Technology*, edited by N. J. Persson (Springer, New York, 2000), illus. 25 cm., 2nd ed.
[21] K. Y. Yasumura, T. D. Stowe, E. M. Chow, T. Pfafman, T. W. Kenny, B. C. Stipe, and D. Rugar, J. Microelectromech. Syst. **9**, 117 (2000).
[22] P. Mohanty, D. A. Harrington, K. L. Ekinci, Y. T. Yang, M. J. Murphy, and M. L. Roukes, Phys. Rev. B **66**, 085416 (2002).